International Journal of Theoretical Physics (2025) 64:316
https://doi.org/10.1007/s10773-025-06171-7

RESEARCH

Advanced Method for Studying Soliton Solutions and Various Solitonic forms of the (3+1)-dimensional Nonlinear Evolution Model

Shubham Kumar Dhiman[1] · Monika Niwas[2] · Sachin Kumar[1] · Wen-Xiu Ma[3,4] · M. A. Abdou[5,6]

Received: 15 July 2025 / Accepted: 9 October 2025 / Published online: 11 November 2025

Abstract
Nonlinear wave models have been widely researched in several relevant scientific disciplines, including theoretical physics, applied mathematics, and plasma physics, over the last 60 years. This research article focuses on deriving several analytical solutions and introduces newly constructed solitonic forms for a nonlinear (3+1)-dimensional evolution equation. The Generalized Exponential Rational Integral Function (GERIF) method is a recently advanced method to investigate exponential, trigonometric, hyperbolic, logarithmic, and inverse function solutions. We visualize these solutions through 3-dimensional (3D), contour, and contour plots to enhance their comprehensibility. These graphical representations show soliton-form solutions, including lumps, peakons, solitons, periodic lumps, periodic peakons, periodic solitons, solitonic wave-patterns, cone shapes, etc. These applications significantly enhance the quality and significance of our work, showcasing the utility of the newly introduced GERIF method. By bridging the gap between theoretical physics, plasma physics, and physical applications, this work presents an entirely new point of view on the evolving multi-soliton and multi-peakon patterns. These findings open the door for future developments in plasma waves and wave propagation while deepening our understanding of complex systems. The obtained forms of graphical representations have not been thoroughly studied in soliton theory up to this point. This research is the first ever to investigate the dynamics of newly generated solutions in plasma physics, nonlinear dynamics, and theoretical physics, incorporating multi-solitons, multi-peakons, and other solitons.

Keywords Mathematical methods · Closed-form solutions · Nonlinear evolution model · Solitons

1 Introduction

During the past six decades, nonlinear wave models have been investigated extensively in theoretical physics, plasma physics, applied mathematics, and other relevant scientific domains [1–3]. Soliton theory, a fundamental concept in mathematical physics, plays a

Extended author information available on the last page of the article

pivotal role in understanding wave phenomena. Its remarkable applications extend to the (3+1)-dimensional evolution equation, where solitons serves as unique solutions, maintaining their shape and energy while propagating through a medium.

In this article, the focus of our study is on the (3+1)-dimensional nonlinear evolution equation, expressed as: [4, 5]:

$$\frac{\partial^2 R}{\partial y\,\partial t} + c_1\left(3\frac{\partial^2 R}{\partial x\,\partial x}\int \frac{\partial R}{\partial y}\,dx + \frac{\partial^4 R}{\partial x\,\partial x\,\partial x\,\partial y} + 3R\frac{\partial^2 R}{\partial x\,\partial y} + 6\frac{\partial R}{\partial x}\frac{\partial R}{\partial y}\right) + c_2\frac{\partial^2 R}{\partial y\,\partial y} + c_3\frac{\partial^2 R}{\partial z\,\partial z} = 0, \quad (1)$$

where c_1, c_2, and c_3 are the real parameters that govern the balance between nonlinearity and dispersion in different spatial directions. This equation is characterized by its intricate structure, involving various partial derivatives and coefficients, reflecting the complexity of wave dynamics in three spatial dimensions. evolution equation plays a significant role in nonlinear wave theory, soliton theory, and various fields of mathematics and physics, where it appears as a key equation that governs the behavior of certain waves and wave-like phenomena. Its solutions provide insights into the complex dynamics of these systems and can have applications in diverse areas such as fluid dynamics, nonlinear optics, and plasma physics. Theoretical analysis of soliton solutions for nonlinear partial differential equations holds significant importance due to its wide-ranging applications. Various effective techniques have been applied to tackle these equations, including the exp-function method [6], Painlevé test [7, 8], Riccati projective equation method [9], the homotopy perturbation method [10], the Adomain decomposition method [11], the inverse (G'/G)-expansion method [12], Lie symmetry method [13], Kudryashov method [14, 15], Hirota bilinear transformation technique [16], the Chamani method [17], the evolution method [18, 19], Lie symmetry method [20], the Galerkin method [21] etc. These methods collectively contribute to a comprehensive toolkit for solving and understanding nonlinear partial differential equations.

We have recently dealt with a few nonlinear evolution problems utilizing a multivariate generalized exponential rational integral function technique [22]. Building on this foundation, we now aim to explore the (3+1)-dimensional evolution equation. This extension provides a more comprehensive understanding of the equation's behavior in higher dimensions. In recent years, various methods have been employed by researchers to investigate the evolution equation, leading to significant advancements in the field. Hosseini et.al [5] examine how dispersive waves behave in the (3+1)-D evolution equation. They employed the Bäcklund transformation and the evolution form, using the truncated Painleve expansion method to extract solutions for this equation. Gunhan and Yasar [23] applied the Painlave integrability concept by utilizing the WTC-Kruskal method and Lie point symmetries to the 3D evolution equation. Additionally, they discussed the conservation law for the consider problem. Ismael et al. [24] adopted the evolution approach along with a long-wave method to investigate various aspects of the 3D evolution equation. They explored multiple M-lump waves, breather waves and its interaction with one soliton.

This article is divided into several sections, each focusing on the Generalized exponential rational integral function method's application to the evolution equation and the resulting outcomes. Section 1 explored the historical origins of the evolution equation, furnishing crucial context to underscore its relevance in the field of nonlinear partial differential equations. In Section 2, we outline the essential steps of the newly introduce "Generalized exponential rational integral function method," presenting a detailed, step-by-step procedure for

obtaining exact solutions to the NLPDE. In Section 3, we applied the Generalized exponential rational integral function method to solve the evolution equation. This approach led us to discover novel solutions to the core problem. To gain a deeper understanding, we visually represented these solutions through graphs, making it possible to identify their relevance in practical scenarios. Furthermore, in Section 4, we visually depict how our solutions behave when different parameters are chosen within an acceptable range. This visual analysis helps us better understand the complexities of nonlinear wave phenomena. In Section 5, we conclude our research study by summarizing the key findings. We emphasize the significant contribution made through the application of the generalized exponential rational function method to the evolution equation. In the last part of our article, we provide a summary of the main points related to future research directions in Section 5.

2 Methodology

Our objective of this section is to highlight the key steps of the Generalized exponential rational integral function (GERIF) method. The GERIF metod's significance lies in its unique ability to provide novel analytic solutions to the nonlinear partial differential Eqs. (NLPDEs). This method is the extension of the already existing method known as generalized exponential rational function (GERF) [25] method and the multiple exp-function method [26].

- A general NLPDEs is

$$F\left(R, \frac{\partial R}{\partial x}, \frac{\partial R}{\partial y}, \frac{\partial R}{\partial z}, \frac{\partial R}{\partial t}, \frac{\partial^2 R}{\partial x^2}, \frac{\partial^2 R}{\partial x \partial t}, \ldots\right) = 0, \tag{2}$$

where $R = R(x, y, z, t)$ is a solution of (2).

- For the reduction of the (2), we are using the transformation

$$R(x, y, z, t) = S(\eta), \ \eta = \omega_1 x + \omega_2 y + \omega_3 z + \omega_4 t + \omega_5, \tag{3}$$

where $\omega_1, \omega_2, \omega_3, \omega_4$ and ω_5 are arbitrary constants. Then the reduced equation can be represent as

$$P(S(\eta), S'(\eta), S''(\eta), \ldots) = 0. \tag{4}$$

- To simplify the above (4), we are assuming a new trial solution of the form

$$S(\eta) = \mathcal{T}_0 + \sum_{i=1}^{N} \mathcal{T}_i \left(\int U(\eta)\, d\eta\right)^i + \sum_{i=1}^{N} \mathcal{K}_i \left(\int U(\eta)\, d\eta\right)^{-i}. \tag{5}$$

Here, $U(\eta)$ is defined as an exponential rational function

$$U(\eta) = \frac{a_1 \exp(b_1\eta) + a_2 \exp(b_2\eta)}{a_3 \exp(b_3\eta) + a_4 \exp(b_4\eta)}. \tag{6}$$

- To ensure that (1) holds true, it is essential to identify suitable values for various parameters like a_j, b_j, $(1 \leq j \leq 4)$, $\mathcal{T}_0$, $\mathcal{T}_i$ and $\mathcal{K}_i$ $(1 \leq i \leq N)$. These parameters must be carefully chosen to ensure that (1) is satisfied perfectly.
- The order of the method depends on *N*, which can be determined by using the balancing principle to both the nonlinear term and the highest order derivative term in the NLODE (4).
- We substitute the expression from (5) into (4) along with (6), yielding an algebraic equation of the form $Q(\Theta_1, \Theta_2, \Theta_3, \Theta_4) = 0$, where, each $\Theta_j = \exp(b_j\eta)$, for $1 \leq j \leq 4$. Subsequently, we will equate each coefficient of the function Q to zero.
- After using software like *Mathematica* for mathematical simplifications, we can find the exact values of the involved variables. Substituting these values into (5) and (6) yields precise exact soliton solutions for (4).

3 Applications of GERIF Method

Here, we utilize the GERIF method to find analytic wave solutions, which include exponential, trigonometric, hyperbolic, logarithmic, and inverse functions, for the evolution equation. Firstly, we employing a wave translation for the (1) in such a way

$$R(x, y, z, t) = S(\eta), \quad \text{with} \quad \eta = \omega_1 x + \omega_2 y + \omega_3 z + \omega_4 t + \omega_5. \tag{7}$$

which reduced the main (1) into the ODE,

$$c_1\omega_2\omega_1^3 S^{(4)}(\eta) + \left(c_2\omega_2^2 + c_3\omega_3^2 + \omega_4\omega_2\right) S''(\eta) + 6c_1\omega_2\omega_1 S(\eta)S''(\eta) + 6c_1\omega_2\omega_1 S'(\eta)^2 = 0. \tag{8}$$

By balancing the terms $S(\eta)^{(4)}$ and $S(\eta)S''(\eta)$ in (8), we determine that $N = 2$. Therefore, the trial solution takes the form

$$S(\eta) = \mathcal{T}_0 + \mathcal{T}_1 \int U(\eta)\, d\eta + \mathcal{T}_2 \left(\int U(\eta)\, d\eta\right)^2 + \frac{\mathcal{K}_1}{\int U(\eta)\, d\eta} + \frac{\mathcal{K}_2}{(\int U(\eta)\, d\eta)^2}. \tag{9}$$

Substituting (9) into (8) and utilizing the GERIF technique via computational software, such as *Mathematica*, yields following sets of solutions along with constraint condition for the evolution equation:

3.1 Exponential Function Form

When the parameters are set as $[a_1, a_2, a_3, a_4] = [2i, 2i, 2i, 2i]$ and $[b_1, b_2, b_3, b_4] = [2, 2, 0, 0]$, (6) simplifies to the standard *exponential* function form

$$U(\eta) = \exp(2\eta). \tag{10}$$

Incorporating the (10) into (9) yields the following form of $S(\eta)$:

$$S(\eta) = \frac{1}{2}\exp(2\eta)\mathcal{T}_1 + \frac{1}{4}\exp(4\eta)\mathcal{T}_2 + 2\exp(-2\eta)\mathcal{K}_1 + 4\exp(-4\eta)\mathcal{K}_2 + \mathcal{T}_0. \quad (11)$$

Case 3.1.1 $$\mathcal{T}_1 \neq 0; \mathcal{K}_1 = 0; \mathcal{T}_2 = 0; \mathcal{K}_2 = 0; c_1 = 0; \omega_4 = \frac{-c_2\omega_2^2 - c_3\omega_3^2}{\omega_2}.$$

A combination of the newly acquired set of constants from the previous (11), solution for (8) recast as

$$S(\eta) = \frac{1}{2}\exp(2\eta)\mathcal{T}_1 + \mathcal{T}_0. \quad (12)$$

We found an exact solution for the evolution (1) by utilizing (12) and (7) as

$$R(x, y, z, t) = \frac{1}{2}\mathcal{T}_1 \exp\left(2\left(\omega_1 x + \omega_2 y + \omega_3 z + \omega_4 t + \omega_5\right)\right) + \mathcal{T}_0. \quad (13)$$

Case 3.1.2 $$\mathcal{T}_0 \neq 0;\ \mathcal{T}_1 \neq 0;\ \mathcal{K}_1 \neq 0;\ \mathcal{T}_2 \neq 0;\ \mathcal{K}_2 \neq 0;\ \omega_1 = 0, \omega_4 = \frac{-c_2\omega_2^2 - c_3\omega_3^2}{\omega_2}.$$

A combination of the newly acquired set of constants from the previous (11), solution for (8) recast as

$$S(\eta) = \frac{1}{2}e^{2\eta}\mathcal{T}_1 + \frac{1}{4}e^{4\eta}\mathcal{T}_2 + \mathcal{T}_0 + 2e^{-2\eta}\mathcal{K}_1 + 4e^{-4\eta}\mathcal{K}_2. \quad (14)$$

We found an exact solution for the evolution (1) by utilizing (14) and (7) as

$$\begin{aligned} R(x, y, z, t) = \mathcal{T}_0 &+ \frac{1}{2}\mathcal{T}_1 \exp\left(2\left(\frac{t\left(-c_2\omega_2^2 - c_3\omega_3^2\right)}{\omega_2} + y\omega_2 + \omega_5 + \omega_3 z\right)\right) \\ &+ \frac{1}{4}\mathcal{T}_2 \exp\left(4\left(\frac{t\left(-c_2\omega_2^2 - c_3\omega_3^2\right)}{\omega_2} + y\omega_2 + \omega_5 + \omega_3 z\right)\right) \\ &+ 2\mathcal{K}_1 \exp\left(-2\left(\frac{t\left(-c_2\omega_2^2 - c_3\omega_3^2\right)}{\omega_2} + y\omega_2 + \omega_5 + \omega_3 z\right)\right) \\ &+ 4\mathcal{K}_2 \exp\left(-4\left(\frac{t\left(-c_2\omega_2^2 - c_3\omega_3^2\right)}{\omega_2} + y\omega_2 + \omega_5 + \omega_3 z\right)\right). \end{aligned} \quad (15)$$

Case 3.1.3 $$\mathcal{T}_1 \neq 0;\ \mathcal{K}_1 \neq 0;\ \mathcal{T}_2 = 0;\ \mathcal{K}_2 = 0;\ \omega_2 = 0.$$

A combination of the newly acquired set of constants from the previous (11), solution for (8) recast as

$$S(\eta) = \frac{1}{2}e^{2\eta}\mathcal{T}_1 + \mathcal{T}_0 + 2e^{-2\eta}\mathcal{K}_1. \tag{16}$$

We found an exact solution for the evolution (1) by utilizing (16) and (7) as

$$R(x,y,z,t) = \frac{1}{2}\mathcal{T}_1 e^{2(t\omega_4 + x\omega_1 + \omega_5 + \omega_3 z)} + \mathcal{T}_0 + 2\mathcal{K}_1 e^{-2(t\omega_4 + x\omega_1 + \omega_5 + \omega_3 z)}. \tag{17}$$

3.2 Sine Function Form

When the parameters are set as $[a_1, a_2, a_3, a_4] = [3/4, -3/4, i, i]$ and $[b_1, b_2, b_3, b_4] = [i, -i, 0, 0]$, (6) simplifies to the standard *sine* function form

$$U(\eta) = \frac{3}{4}\sin(\eta). \tag{18}$$

After substituting (18) into (9), we can determine the form of $S(\eta)$:

$$S(\eta) = \frac{9}{16}\mathcal{T}_2\cos^2(\eta) - \frac{3}{4}\mathcal{T}_1\cos(\eta) + \mathcal{T}_0 + \frac{16}{9}\mathcal{K}_2\sec^2(\eta) - \frac{4}{3}\mathcal{K}_1\sec(\eta). \tag{19}$$

Case 3.2.1 $\mathcal{T}_0 \neq 0;\ \mathcal{T}_1 \neq 0;\ \mathcal{K}_1 \neq 0;\ \mathcal{T}_2 \neq 0;\ \mathcal{K}_2 \neq 0;\ \omega_1 = 0, \omega_4 = \dfrac{-c_2\omega_2^2 - c_3\omega_3^2}{\omega_2}.$

Plugging these constants into (19), we have following solution of ODE (8) as

$$S(\eta) = \frac{9}{16}\mathcal{T}_2\cos^2(\eta) - \frac{3}{4}\mathcal{T}_1\cos(\eta) + \mathcal{T}_0 + \frac{16}{9}\mathcal{K}_2\sec^2(\eta) - \frac{4}{3}\mathcal{K}_1\sec(\eta). \tag{20}$$

Thus, by using (20) within the expression (7), we discover the precise solution to the evolution equation as

$$\begin{aligned} R(x,y,z,t) = {} & \frac{9}{16}\mathcal{T}_2\cos^2\left(\frac{t\left(-c_2\omega_2^2 - c_3\omega_3^2\right)}{\omega_2} + y\omega_2 + \omega_5 + \omega_3 z\right) \\ & - \frac{3}{4}\mathcal{T}_1\cos\left(\frac{t\left(-c_2\omega_2^2 - c_3\omega_3^2\right)}{\omega_2} + y\omega_2 + \omega_5 + \omega_3 z\right) \\ & + \frac{16}{9}\mathcal{K}_2\sec^2\left(\frac{t\left(-c_2\omega_2^2 - c_3\omega_3^2\right)}{\omega_2} + y\omega_2 + \omega_5 + \omega_3 z\right) \\ & - \frac{4}{3}\mathcal{K}_1\sec\left(\frac{t\left(-c_2\omega_2^2 - c_3\omega_3^2\right)}{\omega_2} + y\omega_2 + \omega_5 + \omega_3 z\right) + \mathcal{T}_0. \end{aligned} \tag{21}$$

Case 3.2.2 $\mathcal{T}_0 \neq 0;\ \mathcal{T}_1 \neq 0;\ \mathcal{K}_1 = 0;\ \mathcal{T}_2 \neq 0;\ \mathcal{K}_2 \neq 0;\ c_3 = 0; \omega_2 = 0.$

Plugging these constants into (19), we have following solution of ODE (8) as

$$S(\eta) = \frac{9}{16}\mathcal{T}_2 \cos^2(\eta) - \frac{3}{4}\mathcal{T}_1 \cos(\eta) + \mathcal{T}_0 + \frac{16}{9}\mathcal{K}_2 \sec^2(\eta). \tag{22}$$

Thus, by using (22) within the expression (7), we discover the precise solution to the evolution equation as

$$\begin{aligned} R(x,y,z,t) = {} & \mathcal{T}_0 + \frac{9}{16}\mathcal{T}_2 \cos^2(t\omega_4 + x\omega_1 + \omega_5 + \omega_3 z) - \frac{3}{4}\mathcal{T}_1 \cos(t\omega_4 + x\omega_1 + \omega_5 + \omega_3 z) \\ & + \frac{16}{9}\mathcal{K}_2 \sec^2(t\omega_4 + x\omega_1 + \omega_5 + \omega_3 z). \end{aligned} \tag{23}$$

Case 3.2.3 $\mathcal{T}_0 \neq 0;\ \mathcal{T}_1 \neq 0;\ \mathcal{K}_1 \neq 0;\ \mathcal{T}_2 \neq 0;\ \mathcal{K}_2 \neq 0;\ c_1 = 0;\ \omega_4 = \dfrac{-c_2\omega_2^2 - c_3\omega_3^2}{\omega_2}.$

Plugging these constants into (19), we have following solution of ODE (8) as

$$S(\eta) = \frac{9}{16}\mathcal{T}_2 \cos^2(\eta) - \frac{3}{4}\mathcal{T}_1 \cos(\eta) + \mathcal{T}_0 + \frac{16}{9}\mathcal{K}_2 \sec^2(\eta) - \frac{4}{3}\mathcal{K}_1 \sec(\eta). \tag{24}$$

Thus, by using (24) within the expression (7), we discover the precise solution to the evolution equation as

$$\begin{aligned} R(x,y,z,t) = {} & \frac{9}{16}\mathcal{T}_2 \cos^2(\omega_1 x + \omega_2 y + \omega_3 z + \omega_4 t + \omega_5) - \frac{3}{4}\mathcal{T}_1 \cos(\omega_1 x + \omega_2 y + \omega_3 z + \omega_4 t + \omega_5) \\ & + \frac{16}{9}\mathcal{K}_2 \sec^2(\omega_1 x + \omega_2 y + \omega_3 z + \omega_4 t + \omega_5) - \frac{4}{3}\mathcal{K}_1 \sec(\omega_1 x + \omega_2 y + \omega_3 z + \omega_4 t + \omega_5) + \mathcal{T}_0. \end{aligned} \tag{25}$$

3.3 Cosine Function Form

When the parameters are set as $[a_1, a_2, a_3, a_4] = [i, i, i, i]$ and $[b_1, b_2, b_3, b_4] = [i, -i, 0, 0]$, (6) simplifies to the standard *cosine* function form

$$U(\eta) = \cos(\eta). \tag{26}$$

When we insert (26) into (9), we can express $S(\eta)$ as follows:

$$S(\eta) = \mathcal{T}_2 \sin^2(\eta) + \mathcal{T}_1 \sin(\eta) + \mathcal{T}_0 + \mathcal{K}_2 \csc^2(\eta) + \mathcal{K}_1 \csc(\eta). \tag{27}$$

Case 3.3.1 $\mathcal{T}_0 \neq 0;\ \mathcal{T}_1 \neq 0;\ \mathcal{K}_1 = 0;\ \mathcal{T}_2 \neq 0;\ \mathcal{K}_2 \neq 0;\ \omega_1 = 0;\ \omega_4 = \dfrac{-c_2\omega_2^2 - c_3\omega_3^2}{\omega_2}.$

With the above-mentioned constants applied to (27), the solution for (8) is provided as follows:

$$S(\eta) = \mathcal{T}_2 \sin^2(\eta) + \mathcal{T}_1 \sin(\eta) + \mathcal{T}_0 + \mathcal{K}_2 \csc^2(\eta) + \mathcal{K}_1 \csc(\eta). \tag{28}$$

Hence, from (28) in the context of expression (7), we arrive at the following solution for the evolution equation

$$R(x,y,z,t) = \mathcal{T}_2 \sin^2\left(\frac{t\left(-c_2\omega_2^2 - c_3\omega_3^2\right)}{\omega_2} + y\omega_2 + \omega_5 + \omega_3 z\right) + \mathcal{T}_1 \sin\left(\frac{t\left(-c_2\omega_2^2 - c_3\omega_3^2\right)}{\omega_2} + y\omega_2 + \omega_5 + \omega_3 z\right) + \mathcal{K}_2 \csc^2\left(\frac{t\left(-c_2\omega_2^2 - c_3\omega_3^2\right)}{\omega_2} + y\omega_2 + \omega_5 + \omega_3 z\right) + \mathcal{K}_1 \csc\left(\frac{t\left(-c_2\omega_2^2 - c_3\omega_3^2\right)}{\omega_2} + y\omega_2 + \omega_5 + \omega_3 z\right) + \mathcal{T}_0. \tag{29}$$

Case 3.3.2 $\mathcal{T}_0 \neq 0;\ \mathcal{T}_1 \neq 0;\ \mathcal{K}_1 = 0;\ \mathcal{T}_2 \neq 0;\ \mathcal{K}_2 \neq 0;\ c_3 = 0; \omega_2 = 0.$

With the above-mentioned constants applied to (27), the solution for (8) is provided as follows:

$$S(\eta) = \mathcal{T}_2 \sin^2(\eta) + \mathcal{T}_1 \sin(\eta) + \mathcal{T}_0 + \mathcal{K}_2 \csc^2(\eta). \tag{30}$$

Hence, from (30) in the context of expression (7), we arrive at the following solution for the evolution equation

$$R(x,y,z,t) = \mathcal{T}_2 \sin^2\left(t\omega_4 + x\omega_1 + \omega_5 + \omega_3 z\right) + \mathcal{T}_1 \sin\left(t\omega_4 + x\omega_1 + \omega_5 + \omega_3 z\right) + \mathcal{T}_0 + \mathcal{K}_2 \csc^2\left(t\omega_4 + x\omega_1 + \omega_5 + \omega_3 z\right). \tag{31}$$

Case 3.3.3 $\mathcal{T}_0 \neq 0;\ \mathcal{T}_1 \neq 0;\ \mathcal{K}_1 \neq 0;\ \mathcal{T}_2 \neq 0;\ \mathcal{K}_2 \neq 0;\ c_1 = 0;\ \omega_4 = \dfrac{-c_2\omega_2^2 - c_3\omega_3^2}{\omega_2}.$

With the above-mentioned constants applied to (27), the solution for (8) is provided as follows:

$$S(\eta) = \mathcal{T}_2 \sin^2(\eta) + \mathcal{T}_1 \sin(\eta) + \mathcal{T}_0 + \mathcal{K}_2 \csc^2(\eta) + \mathcal{K}_1 \csc(\eta). \tag{32}$$

Hence, from (32) in the context of expression (7), we arrive at the following solution for the evolution equation

$$R(x,y,z,t) = \mathcal{T}_2 \sin^2\left(\omega_1 x + \omega_2 y + \omega_3 z + \omega_4 t + \omega_5\right) + \mathcal{T}_1 \sin\left(\omega_1 x + \omega_2 y + \omega_3 z + \omega_4 t + \omega_5\right) + \mathcal{K}_2 \csc^2\left(\omega_1 x + \omega_2 y + \omega_3 z + \omega_4 t + \omega_5\right) + \mathcal{K}_1 \csc\left(\omega_1 x + \omega_2 y + \omega_3 z + \omega_4 t + \omega_5\right) + \mathcal{T}_0. \tag{33}$$

3.4 Tangent Function Form

When the parameters are set as $[a_1, a_2, a_3, a_4] = [1, -1, i, i]$ and $[b_1, b_2, b_3, b_4] = [i, -i, i, -i]$, (6) simplifies to the standard *tangent* function form

$$U(\eta) = \tan(\eta). \tag{34}$$

With the above tangent function into (9), we have following form for $S(\eta)$:

$$S(\eta) = \mathcal{T}_2 \log^2(\cos(\eta)) - \mathcal{T}_1 \log(\cos(\eta)) + \mathcal{T}_0 + \frac{\mathcal{K}_2}{\log^2(\cos(\eta))} - \frac{\mathcal{K}_1}{\log(\cos(\eta))}. \tag{35}$$

Case 3.4.1 $\mathcal{T}_0 \neq 0;\ \mathcal{T}_1 \neq 0;\ \mathcal{K}_1 = 0;\ \mathcal{T}_2 = 0;\ \mathcal{K}_2 = 0;\ c_1 = 0;\ \omega_4 = \dfrac{-c_2\omega_2^2 - c_3\omega_3^2}{\omega_2}.$

By substituting the provided constants into (35), we arrive at solution for (8) as follows:

$$S(\eta) = \mathcal{T}_0 - \mathcal{T}_1 \log(\cos(\eta)). \tag{36}$$

Under the (36) and (7), we get

$$R(x, y, z, t) = \mathcal{T}_0 - \mathcal{T}_1 \log\left(\cos\left(\omega_1 x + \omega_2 y + \omega_3 z + \omega_4 t + \omega_5\right)\right). \tag{37}$$

Case 3.4.2 $\mathcal{T}_0 \neq 0;\ \mathcal{T}_1 \neq 0;\ \mathcal{T}_2 \neq 0;\ \mathcal{K}_1 \neq 0;\ \mathcal{K}_2 = 0;\ \omega_1 = 0;\ \omega_4 = \dfrac{-c_2\omega_2^2 - c_3\omega_3^2}{\omega_2}.$

By substituting the provided constants into (35), we arrive at solution for (8) as follows:

$$S(\eta) = \mathcal{T}_0 + \mathcal{T}_2 \log^2(\cos(\eta)) - \mathcal{T}_1 \log(\cos(\eta)) - \frac{\mathcal{K}_1}{\log(\cos(\eta))}. \tag{38}$$

Under the (38) and (7), we have

$$\begin{aligned} R(x, y, z, t) = {} & \mathcal{T}_2 \log^2\left(\cos\left(\omega_2\left(y - c_2 t\right) - \frac{c_3 t\omega_3^2}{\omega_2} + \omega_5 + \omega_3 z\right)\right) \\ & - \mathcal{T}_1 \log\left(\cos\left(\omega_2\left(y - c_2 t\right) - \frac{c_3 t\omega_3^2}{\omega_2} + \omega_5 + \omega_3 z\right)\right) \\ & - \frac{\mathcal{K}_1}{\log\left(\cos\left(\omega_2\left(y - c_2 t\right) - \frac{c_3 t\omega_3^2}{\omega_2} + \omega_5 + \omega_3 z\right)\right)} + \mathcal{T}_0. \end{aligned} \tag{39}$$

Case 3.4.3 $\mathcal{T}_0 \neq 0;\ \mathcal{T}_1 \neq 0;\ \mathcal{K}_1 \neq 0;\ \mathcal{T}_2 \neq 0;\ \mathcal{K}_2 \neq 0;\ c_3 = 0; \omega_2 = 0.$

By substituting the provided constants into (35), we arrive at solution for (8) as follows:

$$S(\eta) = \mathcal{T}_2 \log^2(\cos(\eta)) - \mathcal{T}_1 \log(\cos(\eta)) + \mathcal{T}_0 + \frac{\mathcal{K}_2}{\log^2(\cos(\eta))} - \frac{\mathcal{K}_1}{\log(\cos(\eta))}. \tag{40}$$

Under the (40) and (7), we have

$$\begin{aligned} R(x, y, z, t) = {} & \mathcal{T}_2 \log^2\left(\cos\left(t\omega_4 + x\omega_1 + \omega_5 + \omega_3 z\right)\right) - \mathcal{T}_1 \log\left(\cos\left(t\omega_4 + x\omega_1 + \omega_5 + \omega_3 z\right)\right) + \mathcal{T}_0 \\ & + \frac{\mathcal{K}_2}{\log^2\left(\cos\left(t\omega_4 + x\omega_1 + \omega_5 + \omega_3 z\right)\right)} - \frac{\mathcal{K}_1}{\log\left(\cos\left(t\omega_4 + x\omega_1 + \omega_5 + \omega_3 z\right)\right)}. \end{aligned} \tag{41}$$

3.5 Hyperbolic Sine Function Form

When the parameters are set as $[a_1, a_2, a_3, a_4] = [4i, -4i, 4i, 4i]$ and $[b_1, b_2, b_3, b_4] = [2, -2, 0, 0]$, (6) simplifies to the standard *hyperbolic sine* function form

$$U(\eta) = \sinh(2\eta). \tag{42}$$

When we place (42) in (9), we can define $S(\eta)$ as:

$$S(\eta) = \frac{1}{4}\mathcal{T}_2 \cosh^2(2\eta) + \frac{1}{2}\mathcal{T}_1 \cosh(2\eta) + \mathcal{T}_0 + 4\mathcal{K}_2 \mathrm{sech}^2(2\eta) + 2\mathcal{K}_1 \mathrm{sech}(2\eta). \tag{43}$$

Case 3.5.1 $\mathcal{T}_0 \neq 0;\ \mathcal{T}_1 \neq 0;\ \mathcal{K}_1 = 0;\ \mathcal{T}_2 \neq 0;\ \mathcal{K}_2 \neq 0;\ \omega_1 = 0;\ \omega_4 = \dfrac{-c_2\omega_2^2 - c_3\omega_3^2}{\omega_2}.$

With the constant values outlined in (59), the solution for (8) is

$$S(\eta) = \frac{1}{4}\mathcal{T}_2 \cosh^2(2\eta) + \frac{1}{2}\mathcal{T}_1 \cosh(2\eta) + \mathcal{T}_0 + 4\mathcal{K}_2 \mathrm{sech}^2(2\eta). \tag{44}$$

Equations (44) and (7) lead us to the following solution:

$$\begin{aligned} R(x,y,z,t) = {} & \mathcal{T}_0 + \frac{1}{4}\mathcal{T}_2 \cosh^2\left(2\left(\frac{t\left(-c_2\omega_2^2 - c_3\omega_3^2\right)}{\omega_2} + y\omega_2 + \omega_5 + \omega_3 z\right)\right) \\ & + \frac{1}{2}\mathcal{T}_1 \cosh\left(2\left(\frac{t\left(-c_2\omega_2^2 - c_3\omega_3^2\right)}{\omega_2} + y\omega_2 + \omega_5 + \omega_3 z\right)\right) \\ & + 4\mathcal{K}_2 \mathrm{sech}^2\left(2\left(\frac{t\left(-c_2\omega_2^2 - c_3\omega_3^2\right)}{\omega_2} + y\omega_2 + \omega_5 + \omega_3 z\right)\right). \end{aligned} \tag{45}$$

Case 3.5.2 $\mathcal{T}_0 \neq 0;\ \mathcal{T}_1 \neq 0;\ \mathcal{K}_1 = 0;\ \mathcal{T}_2 \neq 0;\ \mathcal{K}_2 \neq 0;\ c_3 = 0;\ \omega_2 = 0.$

With the constant values outlined in (59), the solution for (8) is

$$S(\eta) = \frac{1}{4}\mathcal{T}_2 \cosh^2(2\eta) + \frac{1}{2}\mathcal{T}_1 \cosh(2\eta) + \mathcal{T}_0 + 4\mathcal{K}_2 \mathrm{sech}^2(2\eta). \tag{46}$$

Equations (46) and (7) lead us to the following solution

$$\begin{aligned} R(x,y,z,t) = {} & \frac{1}{4}\mathcal{T}_2 \cosh^2\left(2\left(t\omega_4 + x\omega_1 + \omega_5 + \omega_3 z\right)\right) + \frac{1}{2}\mathcal{T}_1 \cosh\left(2\left(t\omega_4 + x\omega_1 + \omega_5 + \omega_3 z\right)\right) + \mathcal{T}_0 \\ & + 4\mathcal{K}_2 \mathrm{sech}^2\left(2\left(t\omega_4 + x\omega_1 + \omega_5 + \omega_3 z\right)\right). \end{aligned} \tag{47}$$

Case 3.5.3 $\mathcal{T}_0 \neq 0;\ \mathcal{T}_1 \neq 0;\ \mathcal{K}_1 \neq 0;\ \mathcal{T}_2 \neq 0;\ \mathcal{K}_2 \neq 0;\ c_1 = 0;\ \omega_4 = \dfrac{-c_2\omega_2^2 - c_3\omega_3^2}{\omega_2}.$

With the constant values outlined in (59), the solution for (8) is

$$S(\eta) = \frac{1}{4}\mathcal{T}_2 \cosh^2(2\eta) + \frac{1}{2}\mathcal{T}_1 \cosh(2\eta) + \mathcal{T}_0 + 4\mathcal{K}_2 \mathrm{sech}^2(2\eta) + 2\mathcal{K}_1 \mathrm{sech}(2\eta). \tag{48}$$

Equations (48) and (7) lead us to the following solution

$$R(x,y,z,t) = \frac{1}{4}\mathcal{T}_2 \cosh^2\left(2\left(\omega_1 x + \omega_2 y + \omega_3 z + \omega_4 t + \omega_5\right)\right) + \frac{1}{2}\mathcal{T}_1 \cosh\left(2\left(\omega_1 x + \omega_2 y + \omega_3 z + \omega_4 t + \omega_5\right)\right) + 4\mathcal{K}_2 \mathrm{sech}^2\left(2\left(\omega_1 x + \omega_2 y + \omega_3 z + \omega_4 t + \omega_5\right)\right) + 2\mathcal{K}_1 \mathrm{sech}\left(2\left(\omega_1 x + \omega_2 y + \omega_3 z + \omega_4 t + \omega_5\right)\right) + \mathcal{T}_0. \tag{49}$$

3.6 Hyperbolic Cosecant Function Form

When the parameters are set as $[a_1, a_2, a_3, a_4] = [i, i, -i, i]$ and $[b_1, b_2, b_3, b_4] = [0, 0, -1, 1]$, (6) simplifies to the standard *hyperbolic cosecant* function form

$$U(\eta) = \mathrm{csch}(\eta). \tag{50}$$

After introducing (50) into (9), we arrive at the expression of $S(\eta)$ as:

$$S(\eta) = \mathcal{T}_2\left(\log\left(\sinh\left(\frac{\eta}{2}\right)\right) - \log\left(\cosh\left(\frac{\eta}{2}\right)\right)\right)^2 + \mathcal{T}_1\left(\log\left(\sinh\left(\frac{\eta}{2}\right)\right) - \log\left(\cosh\left(\frac{\eta}{2}\right)\right)\right) + \mathcal{T}_0 + \frac{\mathcal{K}_2}{\left(\log\left(\sinh\left(\frac{\eta}{2}\right)\right) - \log\left(\cosh\left(\frac{\eta}{2}\right)\right)\right)^2} + \frac{\mathcal{K}_1}{\log\left(\sinh\left(\frac{\eta}{2}\right)\right) - \log\left(\cosh\left(\frac{\eta}{2}\right)\right)}. \tag{51}$$

Case 3.6.1 $\mathcal{T}_0 \neq 0;\ \mathcal{T}_1 \neq 0;\ \mathcal{T}_2 = 0;\ \mathcal{K}_1 = 0;\ \mathcal{K}_2 = 0;\ c_1 = 0, \omega_4 = \dfrac{-c_2\omega_2^2 - c_3\omega_3^2}{\omega_2}.$

Plugging these constants into (51), then we get the following solution

$$S(\eta) = \mathcal{T}_1\left(\log\left(\sinh\left(\frac{\eta}{2}\right)\right) - \log\left(\cosh\left(\frac{\eta}{2}\right)\right)\right) + \mathcal{T}_0. \tag{52}$$

Accordingly, the evolution equation has the following exact solution

$$R(x,y,z,t) = \mathcal{T}_1 \log\left(\sinh\left(\frac{1}{2}\left(\omega_1 x + \omega_2 y + \omega_3 z + \omega_4 t + \omega_5\right)\right)\right) - \mathcal{T}_1 \log\left(\cosh\left(\frac{1}{2}\left(\omega_1 x + \omega_2 y + \omega_3 z + \omega_4 t + \omega_5\right)\right)\right) + \mathcal{T}_0. \tag{53}$$

Case 3.6.2 $\mathcal{T}_0 \neq 0;\ \mathcal{T}_1 \neq 0;\ \mathcal{T}_2 \neq 0;\ \mathcal{K}_1 \neq 0;\ \mathcal{K}_2 \neq 0;\ \omega_1 = 0;\ \omega_4 = \dfrac{-c_2\omega_2^2 - c_3\omega_3^2}{\omega_2}.$

Plugging these constants into (51), then we get the following solution

$$S(\eta) = \mathcal{T}_2\left(\log\left(\sinh\left(\frac{\eta}{2}\right)\right) - \log\left(\cosh\left(\frac{\eta}{2}\right)\right)\right)^2 + \mathcal{T}_1\left(\log\left(\sinh\left(\frac{\eta}{2}\right)\right) - \log\left(\cosh\left(\frac{\eta}{2}\right)\right)\right) + \mathcal{T}_0 + \frac{\mathcal{K}_2}{\left(\log\left(\sinh\left(\frac{\eta}{2}\right)\right) - \log\left(\cosh\left(\frac{\eta}{2}\right)\right)\right)^2} + \frac{\mathcal{K}_1}{\log\left(\sinh\left(\frac{\eta}{2}\right)\right) - \log\left(\cosh\left(\frac{\eta}{2}\right)\right)}. \tag{54}$$

Accordingly, the evolution equation has the following exact solution

$$
\begin{aligned}
R(x,y,z,t) &= \mathcal{T}_2 \log^2\left(\sinh\left(\frac{1}{2}\left(t\omega_4 + y\omega_2 + \omega_5 + \omega_3 z\right)\right)\right) + \mathcal{T}_1 \log\left(\sinh\left(\frac{1}{2}\left(t\omega_4 + y\omega_2 + \omega_5 + \omega_3 z\right)\right)\right) \\
&+ \mathcal{T}_2 \log^2\left(\cosh\left(\frac{1}{2}\left(t\omega_4 + y\omega_2 + \omega_5 + \omega_3 z\right)\right)\right) - \mathcal{T}_1 \log\left(\cosh\left(\frac{1}{2}\left(t\omega_4 + y\omega_2 + \omega_5 + \omega_3 z\right)\right)\right) \\
&- 2\mathcal{T}_2 \log\left(\sinh\left(\frac{1}{2}\left(t\omega_4 + y\omega_2 + \omega_5 + \omega_3 z\right)\right)\right) \log\left(\cosh\left(\frac{1}{2}\left(t\omega_4 + y\omega_2 + \omega_5 + \omega_3 z\right)\right)\right) \\
&+ \frac{\mathcal{K}_1}{\log\left(\sinh\left(\frac{1}{2}\left(t\omega_4 + y\omega_2 + \omega_5 + \omega_3 z\right)\right)\right) - \log\left(\cosh\left(\frac{1}{2}\left(t\omega_4 + y\omega_2 + \omega_5 + \omega_3 z\right)\right)\right)} \\
&+ \frac{\mathcal{K}_2}{\left(\log\left(\sinh\left(\frac{1}{2}\left(t\omega_4 + y\omega_2 + \omega_5 + \omega_3 z\right)\right)\right) - \log\left(\cosh\left(\frac{1}{2}\left(t\omega_4 + y\omega_2 + \omega_5 + \omega_3 z\right)\right)\right)\right)^2} + \mathcal{T}_0.
\end{aligned} \tag{55}
$$

Case 3.6.3 $\mathcal{T}_0 \neq 0;\ \mathcal{T}_1 \neq 0;\ \mathcal{K}_1 \neq 0;\ \mathcal{T}_2 \neq 0;\ \mathcal{K}_2 \neq 0;\ c_1 = 0;\ \omega_4 = \dfrac{-c_2\omega_2^2 - c_3\omega_3^2}{\omega_2}.$

Plugging these constants into (51), then we get the following solution

$$
\begin{aligned}
S(\eta) &= \mathcal{T}_2\left(\log\left(\sinh\left(\frac{\eta}{2}\right)\right) - \log\left(\cosh\left(\frac{\eta}{2}\right)\right)\right)^2 + \mathcal{T}_1\left(\log\left(\sinh\left(\frac{\eta}{2}\right)\right) - \log\left(\cosh\left(\frac{\eta}{2}\right)\right)\right) + \mathcal{T}_0 \\
&+ \frac{\mathcal{K}_2}{\left(\log\left(\sinh\left(\frac{\eta}{2}\right)\right) - \log\left(\cosh\left(\frac{\eta}{2}\right)\right)\right)^2} + \frac{\mathcal{K}_1}{\log\left(\sinh\left(\frac{\eta}{2}\right)\right) - \log\left(\cosh\left(\frac{\eta}{2}\right)\right)}.
\end{aligned} \tag{56}
$$

Accordingly, the evolution equation has the following exact solution

$$
\begin{aligned}
R(x,y,z,t) &= \mathcal{T}_2 \log^2\left(\sinh\left(\frac{1}{2}\left(\omega_1 x + \omega_2 y + \omega_3 z + \omega_4 t + \omega_5\right)\right)\right) \\
&+ \mathcal{T}_1 \log\left(\sinh\left(\frac{1}{2}\left(\omega_1 x + \omega_2 y + \omega_3 z + \omega_4 t + \omega_5\right)\right)\right) \\
&+ \mathcal{T}_2 \log^2\left(\cosh\left(\frac{1}{2}\left(\omega_1 x + \omega_2 y + \omega_3 z + \omega_4 t + \omega_5\right)\right)\right) \\
&- \mathcal{T}_1 \log\left(\cosh\left(\frac{1}{2}\left(\omega_1 x + \omega_2 y + \omega_3 z + \omega_4 t + \omega_5\right)\right)\right) \\
&- 2\mathcal{T}_2 \log\left(\sinh\left(\frac{1}{2}\left(\omega_1 x + \omega_2 y + \omega_3 z + \omega_4 t + \omega_5\right)\right)\right) \\
&\log\left(\cosh\left(\frac{1}{2}\left(\omega_1 x + \omega_2 y + \omega_3 z + \omega_4 t + \omega_5\right)\right)\right) + \mathcal{T}_0 \\
&+ \frac{\mathcal{K}_1}{\log\left(\sinh\left(\frac{1}{2}\left(\omega_1 x + \omega_2 y + \omega_3 z + \omega_4 t + \omega_5\right)\right)\right) - \log\left(\cosh\left(\frac{1}{2}\left(\omega_1 x + \omega_2 y + \omega_3 z + \omega_4 t + \omega_5\right)\right)\right)} \\
&+ \frac{\mathcal{K}_2}{\left(\log\left(\cosh\left(\frac{1}{2}\left(\omega_1 x + \omega_2 y + \omega_3 z + \omega_4 t + \omega_5\right)\right)\right) - \log\left(\sinh\left(\frac{1}{2}\left(\omega_1 x + \omega_2 y + \omega_3 z + \omega_4 t + \omega_5\right)\right)\right)\right)^2}.
\end{aligned} \tag{57}
$$

3.7 Hyperbolic Secant Function Form:

When the parameters are set as $[a_1, a_2, a_3, a_4] = [2, 2, 2, 2]$ and $[b_1, b_2, b_3, b_4] = [0, 0, 1, -1]$, (6) simplifies to the standard *hyperbolic secant* function form

$$U(\eta) = \operatorname{sech}(\eta). \tag{58}$$

Above secant hyperbolic function along with (9) establish the following form for $S(\eta)$:

$$S(\eta) = 4\mathcal{T}_2 \tan^{-1}\left(\tanh\left(\frac{\eta}{2}\right)\right)^2 + 2\mathcal{T}_1 \tan^{-1}\left(\tanh\left(\frac{\eta}{2}\right)\right) + \mathcal{T}_0 + \frac{\mathcal{K}_1}{2\tan^{-1}\left(\tanh\left(\frac{\eta}{2}\right)\right)} + \frac{\mathcal{K}_2}{4\tan^{-1}\left(\tanh\left(\frac{\eta}{2}\right)\right)^2}. \tag{59}$$

Case 3.7.1: $\mathcal{T}_0 \neq 0;\ \mathcal{T}_1 \neq 0;\ \mathcal{K}_1 = 0;\ \mathcal{T}_2 = 0;\ \mathcal{K}_2 = 0;\ c_1 = 0;\ \omega_4 = \dfrac{-c_2\omega_2^2 - c_3\omega_3^2}{\omega_2}.$

With the constant values outlined in (59), the solution for (8) is

$$S(\eta) = 2\mathcal{T}_1 \tan^{-1}\left(\tanh\left(\frac{\eta}{2}\right)\right) + \mathcal{T}_0. \tag{60}$$

Hence, (60) and (7) provide us a soliton solution of evolution equation as

$$R(x,y,z,t) = 2\mathcal{T}_1 \tan^{-1}\left(\tanh\left(\frac{1}{2}\left(\omega_1 x + \omega_2 y + \omega_3 z + \omega_4 t + \omega_5\right)\right)\right) + \mathcal{T}_0. \tag{61}$$

Case 3.7.2 $\mathcal{T}_0 \neq 0;\ \mathcal{T}_1 \neq 0;\ \mathcal{K}_1 \neq 0;\ \mathcal{T}_2 \neq 0;\ \mathcal{K}_2 \neq 0;\ \omega_1 = 0;\ \omega_4 = \dfrac{-c_2\omega_2^2 - c_3\omega_3^2}{\omega_2}.$

With the constant values outlined in (59), the solution for (8) is

$$S(\eta) = \mathcal{T}_0 + 4\mathcal{T}_2 \tan^{-1}\left(\tanh\left(\frac{\eta}{2}\right)\right)^2 + 2\mathcal{T}_1 \tan^{-1}\left(\tanh\left(\frac{\eta}{2}\right)\right) + \frac{\mathcal{K}_1}{2\tan^{-1}\left(\tanh\left(\frac{\eta}{2}\right)\right)} + \frac{\mathcal{K}_2}{4\tan^{-1}\left(\tanh\left(\frac{\eta}{2}\right)\right)^2}. \tag{62}$$

Hence, (62) and (7) provide us a soliton solution of evolution equation as

$$\begin{aligned} R(x,y,z,t) &= 4\mathcal{T}_2 \tan^{-1}\left(\tanh\left(\frac{1}{2}\left(t\omega_4 + y\omega_2 + \omega_5 + \omega_3 z\right)\right)\right)^2 + 2\mathcal{T}_1 \tan^{-1}\left(\tanh\left(\frac{1}{2}\left(t\omega_4 + y\omega_2 + \omega_5 + \omega_3 z\right)\right)\right) \\ &+ \frac{\mathcal{K}_1}{2\tan^{-1}\left(\tanh\left(\frac{1}{2}\left(t\omega_4 + y\omega_2 + \omega_5 + \omega_3 z\right)\right)\right)} + \frac{\mathcal{K}_2}{4\tan^{-1}\left(\tanh\left(\frac{1}{2}\left(t\omega_4 + y\omega_2 + \omega_5 + \omega_3 z\right)\right)\right)^2} + \mathcal{T}_0. \end{aligned} \tag{63}$$

Case 3.7.3 $\mathcal{T}_0 \neq 0;\ \mathcal{T}_1 \neq 0;\ \mathcal{K}_1 \neq 0;\ \mathcal{T}_2 \neq 0;\ \mathcal{K}_2 \neq 0;\ c_1 = 0;\ \omega_4 = \dfrac{-c_2\omega_2^2 - c_3\omega_3^2}{\omega_2}.$

With the constant values outlined in (59), the solution for (8) is

$$S(\eta) = 4\mathcal{T}_2 \tan^{-1}\left(\tanh\left(\frac{\eta}{2}\right)\right)^2 + 2\mathcal{T}_1 \tan^{-1}\left(\tanh\left(\frac{\eta}{2}\right)\right) + \mathcal{T}_0 + \frac{\mathcal{K}_1}{2\tan^{-1}\left(\tanh\left(\frac{\eta}{2}\right)\right)} + \frac{\mathcal{K}_2}{4\tan^{-1}\left(\tanh\left(\frac{\eta}{2}\right)\right)^2}. \tag{64}$$

Hence, (64) and (7) provide us a soliton solution of evolution equation as

$$\begin{aligned} R(x,y,z,t) &= 4\mathcal{T}_2 \tan^{-1}\left(\tanh\left(\frac{1}{2}\left(\omega_1 x + \omega_2 y + \omega_3 z + \omega_4 t + \omega_5\right)\right)\right)^2 + \mathcal{T}_0 \\ &+ 2\mathcal{T}_1 \tan^{-1}\left(\tanh\left(\frac{1}{2}\left(\omega_1 x + \omega_2 y + \omega_3 z + \omega_4 t + \omega_5\right)\right)\right) + \frac{\mathcal{K}_1}{2\tan^{-1}\left(\tanh\left(\frac{1}{2}\left(\omega_1 x + \omega_2 y + \omega_3 z + \omega_4 t + \omega_5\right)\right)\right)} \\ &+ \frac{\mathcal{K}_2}{4\tan^{-1}\left(\tanh\left(\frac{1}{2}\left(\omega_1 x + \omega_2 y + \omega_3 z + \omega_4 t + \omega_5\right)\right)\right)^2}. \end{aligned} \tag{65}$$

3.8 Hyperbolic Tangent Function Form

When the parameters are set as $[a_1, a_2, a_3, a_4] = [1, -1, 1, 1]$ and $[b_1, b_2, b_3, b_4] = [1, -1, 1, -1]$, (6) simplifies to the standard *hyperbolic tangent* function form

$$U(\eta) = \tanh(\eta). \tag{66}$$

The following expression for $S(\eta)$ is attained by inserting (66) into (9):

$$S(\eta) = \mathcal{T}_2 \log^2(\cosh(\eta)) + \mathcal{T}_1 \log(\cosh(\eta)) + \mathcal{T}_0 + \frac{\mathcal{K}_2}{\log^2(\cosh(\eta))} + \frac{\mathcal{K}_1}{\log(\cosh(\eta))}. \tag{67}$$

Case 3.8.1 $\mathcal{T}_0 \neq 0;\ \mathcal{T}_1 \neq 0;\ \mathcal{K}_1 = 0;\ \mathcal{T}_2 = 0;\ \mathcal{K}_2 = 0;\ c_1 = 0;\ \omega_4 = \dfrac{-c_2\omega_2^2 - c_3\omega_3^2}{\omega_2}.$

Thus, these constants provide us the following solution to the ODE (8),

$$S(\eta) = \mathcal{T}_1 \log(\cosh(\eta)) + \mathcal{T}_0. \tag{68}$$

The above solution of ODE under the transformation (7) gives us the following solution of evolution equation

$$R(x, y, z, t) = \mathcal{T}_1 \log\left(\cosh\left(\omega_1 x + \omega_2 y + \omega_3 z + \omega_4 t + \omega_5\right)\right) + \mathcal{T}_0. \tag{69}$$

Case 3.8.2 $\mathcal{T}_0 \neq 0;\ \mathcal{T}_1 \neq 0;\ \mathcal{T}_2 \neq 0;\ \mathcal{K}_1 \neq 0;\ \mathcal{K}_2 \neq 0;\ \omega_1 = 0;\ \omega_4 = \dfrac{-c_2\omega_2^2 - c_3\omega_3^2}{\omega_2}.$

Thus, these constants provide us the following solution to the ODE (8),

$$S(\eta) = \mathcal{T}_2 \log^2(\cosh(\eta)) + \mathcal{T}_1 \log(\cosh(\eta)) + \mathcal{T}_0 + \frac{\mathcal{K}_2}{\log^2(\cosh(\eta))} + \frac{\mathcal{K}_1}{\log(\cosh(\eta))}. \tag{70}$$

The above solution of ODE under the transformation (7) gives us the following solution of evolution equation

$$\begin{aligned} R(x, y, z, t) = {} & \mathcal{T}_2 \log^2\left(\cosh\left(t\omega_4 + y\omega_2 + \omega_5 + \omega_3 z\right)\right) + \mathcal{T}_1 \log\left(\cosh\left(t\omega_4 + y\omega_2 + \omega_5 + \omega_3 z\right)\right) \\ & + \frac{\mathcal{K}_2}{\log^2\left(\cosh\left(t\omega_4 + y\omega_2 + \omega_5 + \omega_3 z\right)\right)} + \frac{\mathcal{K}_1}{\log\left(\cosh\left(t\omega_4 + y\omega_2 + \omega_5 + \omega_3 z\right)\right)} + \mathcal{T}_0. \end{aligned} \tag{71}$$

Case 3.8.3 $\mathcal{T}_0 \neq 0;\ \mathcal{T}_1 \neq 0;\ \mathcal{K}_1 = 0;\ \mathcal{T}_2 \neq 0;\ \mathcal{K}_2 = 0;\ c_3 = 0;\ \omega_2 = 0.$

Thus, these constants provide us the following solution to the ODE (8),

$$S(\eta) = \mathcal{T}_2 \log^2(\cosh(\eta)) + \mathcal{T}_1 \log(\cosh(\eta)) + \mathcal{T}_0. \tag{72}$$

The above solution of ODE under the transformation (7) gives us the following solution of evolution equation

$$R(x,y,z,t) = \mathcal{T}_2 \log^2\left(\cosh\left(t\omega_4 + x\omega_1 + \omega_5 + \omega_3 z\right)\right) + \mathcal{T}_1 \log\left(\cosh\left(t\omega_4 + x\omega_1 + \omega_5 + \omega_3 z\right)\right) + \mathcal{T}_0. \quad (73)$$

3.9 Hyperbolic Cotangent Function Form

When the parameters are set as $[a_1, a_2, a_3, a_4] = [1, 1, 1, -1]$ and $[b_1, b_2, b_3, b_4] = [1, -1, 1, -1]$, (6) simplifies to the standard *hyperbolic cotangent* function form

$$U(\eta) = \coth(\eta). \quad (74)$$

Placing above expression of $U(\eta)$ into (9), then the form of $S(\eta)$ is given by

$$S(\eta) = \mathcal{T}_2 \log^2(\sinh(\eta)) + \mathcal{T}_1 \log(\sinh(\eta)) + \mathcal{T}_0 + \frac{\mathcal{K}_2}{\log^2(\sinh(\eta))} + \frac{\mathcal{K}_1}{\log(\sinh(\eta))}. \quad (75)$$

Case 3.9.1 $\mathcal{T}_0 \neq 0;\ \mathcal{T}_1 \neq 0;\ \mathcal{K}_1 = 0;\ \mathcal{T}_2 = 0;\ \mathcal{K}_2 = 0;\ c_1 = 0;\ \omega_4 = \dfrac{-c_2\omega_2^2 - c_3\omega_3^2}{\omega_2}.$

With these constants incorporated into (75), a solution for the ODE (8) can be established as

$$S(\eta) = \mathcal{T}_1 \log(\sinh(\eta)) + \mathcal{T}_0. \quad (76)$$

Use of (76) and (7) provide us the following solution

$$R(x,y,z,t) = \mathcal{T}_1 \log\left(\sinh\left(\omega_1 x + \omega_2 y + \omega_3 z + \omega_4 t + \omega_5\right)\right) + \mathcal{T}_0. \quad (77)$$

Case 3.9.2 $\mathcal{T}_0 \neq 0;\ \mathcal{T}_1 \neq 0;\ \mathcal{K}_1 = 0;\ \mathcal{T}_2 \neq 0;\ \mathcal{K}_2 = 0;\ c_3 = 0;\ \omega_2 = 0.$

With these constants incorporated into (75), a solution for the ODE (8) can be established as

$$S(\eta) = \mathcal{T}_2 \log^2(\sinh(\eta)) + \mathcal{T}_1 \log(\sinh(\eta)) + \mathcal{T}_0. \quad (78)$$

Use of (78) and (7) provide us the following solution

$$R(x,y,z,t) = \mathcal{T}_2 \log^2\left(\sinh\left(t\omega_4 + x\omega_1 + \omega_5 + \omega_3 z\right)\right) + \mathcal{T}_1 \log\left(\sinh\left(t\omega_4 + x\omega_1 + \omega_5 + \omega_3 z\right)\right) + \mathcal{T}_0. \quad (79)$$

Case 3.9.3 $\mathcal{T}_0 \neq 0;\ \mathcal{T}_1 \neq 0;\ \mathcal{T}_2 \neq 0;\ \mathcal{K}_1 \neq 0;\ \mathcal{K}_2 \neq 0;\ \omega_1 = 0;\ \omega_4 = \dfrac{-c_2\omega_2^2 - c_3\omega_3^2}{\omega_2}.$

With these constants incorporated into (75), a solution for the ODE (8) can be established as

$$S(\eta) = \mathcal{T}_2 \log^2(\sinh(\eta)) + \mathcal{T}_1 \log(\sinh(\eta)) + \mathcal{T}_0 + \frac{\mathcal{K}_2}{\log^2(\sinh(\eta))} + \frac{\mathcal{K}_1}{\log(\sinh(\eta))}. \quad (80)$$

Use of (80) and (7) provide us the following solution

$$R(x,y,z,t) = \mathcal{T}_2 \log^2\left(\sinh\left(t\omega_4 + y\omega_2 + \omega_5 + \omega_3 z\right)\right) + \mathcal{T}_1 \log\left(\sinh\left(t\omega_4 + y\omega_2 + \omega_5 + \omega_3 z\right)\right) + \frac{\mathcal{K}_2}{\log^2\left(\sinh\left(t\omega_4 + y\omega_2 + \omega_5 + \omega_3 z\right)\right)} + \frac{\mathcal{K}_1}{\log\left(\sinh\left(t\omega_4 + y\omega_2 + \omega_5 + \omega_3 z\right)\right)} + \mathcal{T}_0. \tag{81}$$

4 Graphical Discussion

- Figure 1 provides a visual representation of peakons, lumps and solitons for the solution (25). Here (a) 3D plot of the real part, illustrating the spatial distribution and amplitude peaks for $\omega_1 = 1$, $\omega_2 = 5i$, $\omega_3 = i$, $\omega_5 = 0$, $\mathcal{T}_0 = 1$, $\mathcal{T}_1 = 0$, $\mathcal{T}_2 = 1$, $\mathcal{K}_1 = 2$, $\mathcal{K}_2 = 1$, with time and spatial coordinates set to $t = 0.1, z = 0.02$. The plot covers a specified range of values, with $x \in [-4, 3]$ and $y \in [0.3, 0.3]$, (b) 3D plot of the imaginary part, showing the variation and amplitude peaks in the imaginary component for $\omega_1 = 1$, $\omega_2 = 5i$, $\omega_3 = i$, $\omega_5 = 0$, $\mathcal{T}_0 = 1$, $\mathcal{T}_1 = 0$, $\mathcal{T}_2 = 1$, $\mathcal{K}_1 = 1$, $\mathcal{K}_2 = 1$, with time and spatial coordinates set to $t = 0.01, z = 0.02$ within the bounds of $x \in [-4, 3]$ and $y \in [0.3, 0.3]$, (c) 3D plot of the magnitude, depicting the combined amplitude of real and imaginary parts for $\omega_1 = 2$, $\omega_2 = 5i$, $\omega_3 = i$, $\omega_5 = 0$, $\mathcal{T}_0 = 1$, $\mathcal{T}_1 = 0$, $\mathcal{T}_2 = 0$, $\mathcal{K}_1 = 2$, $\mathcal{K}_2 = 0$, with time and spatial coordinates set to $t = 0.1, z = -0.02$ within the bounds of $x \in [-3.5, 2.6]$ and $y \in [-0.5, 0.5]$, subgraphs (d) highlighting the intricate pattern and symmetry in the real component, (e) showcasing the detailed structure and distribution in the imaginary component and (f) illustrating the overall amplitude patterns and their spatial arrangement.
- Figure 2 showcases the behavior of periodic-soliton, lumps and solitons in the context of the solution (25). (a) 3D plot of the real part, showcasing the spatial distribution and amplitude variations with distinct peaks for $\omega_1 = 2$, $\omega_2 = 2i$, $\omega_3 = i$, $\omega_5 = 0$, $\mathcal{T}_0 = 0$, $\mathcal{T}_1 = 0.01$, $\mathcal{T}_2 = 1$, $\mathcal{K}_1 = 2$, $\mathcal{K}_2 = 1$, with time and spatial coordinates set to

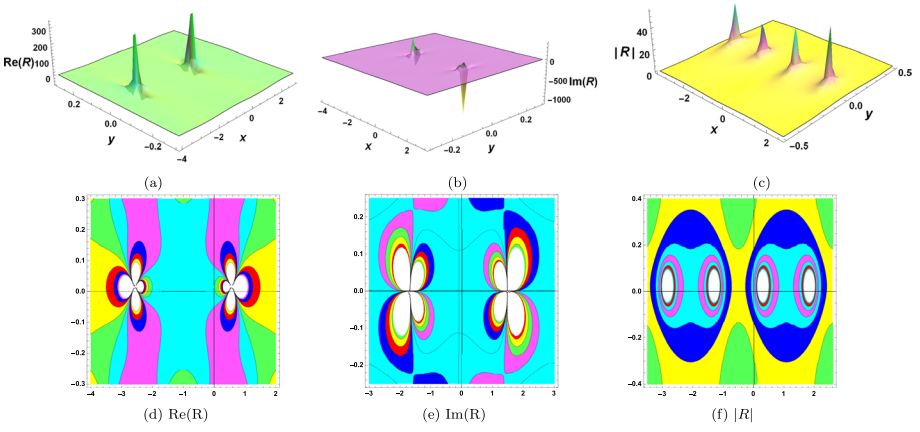

Fig. 1 Visual illustrations, incorporating 3D and contour graphs, of the real, imaginary, and magnitude components of (25) representing the peakons, lumps and solitons

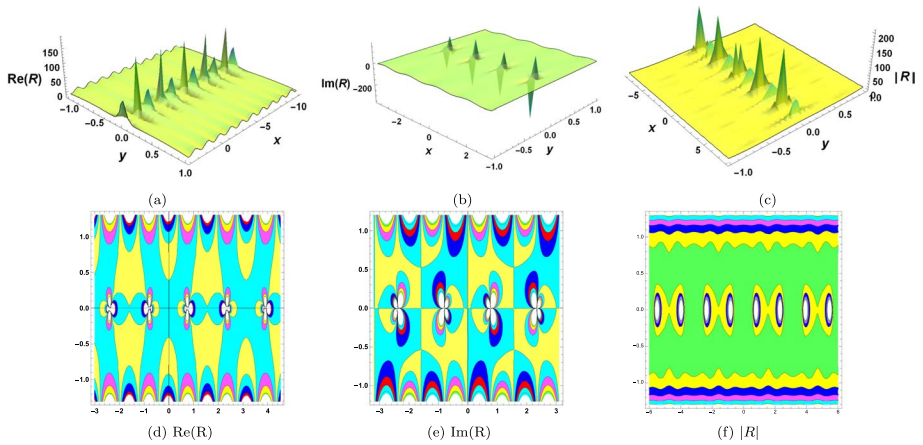

Fig. 2 Visual illustrations, incorporating 3D and contour graphs, of the real, imaginary, and magnitude components of (25) which describes the symmetric behavior

$t = 0.01, z = 0.04$ within the bounds of $x \in [-12, 4]$ and $y \in [-1, 1]$, (b) illustrating the variation and notable peaks in the imaginary component for $\omega_1 = 2$, $\omega_2 = 2i$, $\omega_3 = i$, $\omega_5 = 0$, $\mathcal{T}_0 = 0$, $\mathcal{T}_1 = 0.01$, $\mathcal{T}_2 = 1$, $\mathcal{K}_1 = 2$, $\mathcal{K}_2 = 1$, with time and spatial coordinates set to $t = 0.01, z = 0.04$ within the bounds of $x \in [-3.2, 3.1]$ and $y \in [-1, 1]$, (c) depicting the combined amplitude of the real and imaginary parts with prominent peaks for $\omega_1 = 2, \omega_2 = 2i, \omega_3 = i, \omega_5 = 0, \mathcal{T}_0 = 0, \mathcal{T}_1 = 0.01, \mathcal{T}_2 = 1, \mathcal{K}_1 = 2, \mathcal{K}_2 = 1$, with time and spatial coordinates set to $t = 0.01, z = 0.03$ within the bounds of $x \in [-8, 8]$ and $y \in [-1, 1]$, subgraphs (d), (e) and (f) depict the associated contour plots.

- Figure 3 provides a visual representation of lumps, and multi-solitons in the solution (33). (a) The surface appears to have several peaks and valleys, indicating regions of positive and negative values of Re (R) for $\omega_1 = 2$, $\omega_2 = 5i$, $\omega_3 = i$, $\omega_5 = 0$, $\mathcal{T}_0 = 1$, $\mathcal{T}_1 = 0$,

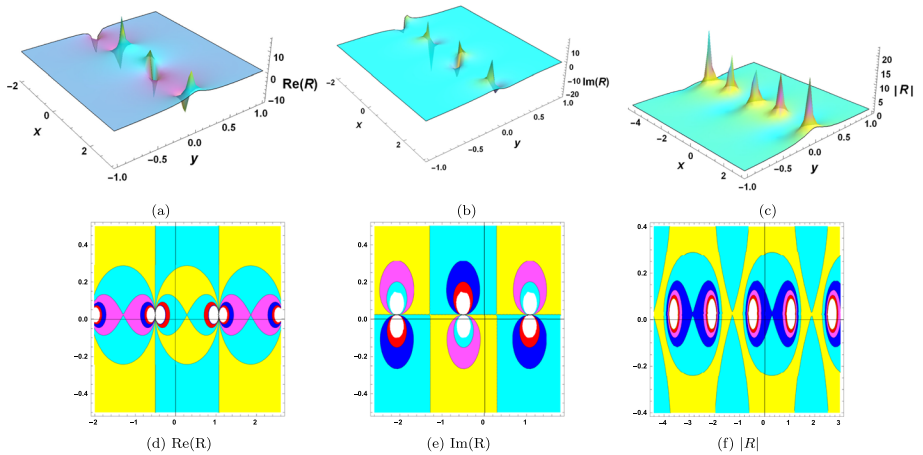

Fig. 3 Visualization of (33): real and imaginary parts reveal oscillatory behavior, while the magnitude indicates localized intensity distributions

$\mathcal{T}_2 = 0$, $\mathcal{K}_1 = 2$, $\mathcal{K}_2 = 0$, with time and spatial coordinates set to $t = 0.1, z = -0.02$ within the bounds of $x \in [-2, 3]$ and $y \in [-1, 1]$, (b) The surface has distinct peaks and troughs, suggesting varying imaginary values across the xy-plane for $\omega_1 = 2$, $\omega_2 = 5i$, $\omega_3 = i$, $\omega_5 = 0$, $\mathcal{T}_0 = 1$, $\mathcal{T}_1 = 0$, $\mathcal{T}_2 = 0$, $\mathcal{K}_1 = 2$, $\mathcal{K}_2 = 0$, with time and spatial coordinates set to $t = 0.1, z = -0.02$ within the bounds of $x \in [-2, 3]$ and $y \in [-1, 1]$, (c) The surface has sharp peaks, indicating regions where $|R|$ is significantly large. Here, $\omega_1 = 2$, $\omega_2 = 5i$, $\omega_3 = i$, $\omega_5 = 0$, $\mathcal{T}_0 = 1$, $\mathcal{T}_1 = 0$, $\mathcal{T}_2 = 0$, $\mathcal{K}_1 = 2$, $\mathcal{K}_2 = 0$, with time and spatial coordinates set to $t = 0.1, z = -0.02$ within the bounds of $x \in [-4.4, 3]$ and $y \in [-1, 1]$, subgraphs (d), (e) and (f) depict the associated contour plots, peaks in the magnitude are represented by closed contours.

- Figure 4 illustrates the presence of peakons, lumps and solitons described by (49), under specific parametric values: (a) $\omega_1 = 1$, $\omega_2 = i$, $\omega_3 = 0.2i$, $\omega_5 = 0.2$, $\mathcal{T}_0 = 0$, $\mathcal{T}_1 = 0$, $\mathcal{T}_2 = 0$, $\mathcal{K}_1 = 2$, $\mathcal{K}_2 = 3$, with time and spatial coordinates set to $t = 0.01, z = 0.01$ within the bounds of $x \in [-1.5, 1.3]$ and $y \in [-2, 2]$, (b) $\omega_1 = 1$, $\omega_2 = i$, $\omega_3 = 2i$, $\omega_5 = 0.2$, $\mathcal{T}_0 = 0$, $\mathcal{T}_1 = 0$, $\mathcal{T}_2 = 0$, $\mathcal{K}_1 = 2$, $\mathcal{K}_2 = 3$, with time and spatial coordinates set to $t = 0.01, z = 0.02$ within the bounds of $x \in [-1.5, 1.3]$ and $y \in [-1.8, 2]$, (c) $\omega_1 = 1, \omega_2 = i, \omega_3 = 2i, \omega_5 = 0.2, \mathcal{T}_0 = 0, \mathcal{T}_1 = 0, \mathcal{T}_2 = 0, \mathcal{K}_1 = 2, \mathcal{K}_2 = 3$, with time and spatial coordinates set to $t = 0.01, z = 0.02$ within the bounds of $x \in [-1.5, 1.3]$ and $y \in [-1.8, 2]$, subgraphs (d), (e) and (f) depict the associated contour plots.
- Figure 5 shows the variation in the behavior of of the solution (61), based on specified choice of parameters. (a) showing a smooth surface with subtle peaks and valleys for $\omega_1 = 2$, $\omega_2 = 7i$, $\omega_3 = i$, $\omega_5 = 0$, $\mathcal{T}_0 = 1$, $\mathcal{T}_1 = 0.01$, with time and spatial coordinates set to $t = 0.001, z = 0.002$ within the bounds of $x \in [-1, 1]$ and $y \in [-0.2, 0.2]$, (b) presenting a similar smooth surface with minor variations for $\omega_1 = 1.7, \omega_2 = 5i, \omega_3 = i$, $\omega_5 = 0$, $\mathcal{T}_0 = 1$, $\mathcal{T}_1 = 0.01$, with time and spatial coordinates set to $t = 0.01, z = 0.02$ within the bounds of $x \in [-2, 2]$ and $y \in [-0.2, 0.2]$, (c) highlighting distinct peaks on the surface for $\omega_1 = 1.7$, $\omega_2 = 5i$, $\omega_3 = i$, $\omega_5 = 0$, $\mathcal{T}_0 = 0.1$, $\mathcal{T}_1 = 0.01$, with time and spatial coordinates set to $t = 0.02, z = 0.02$ within the bounds of $x \in [-1, 1]$ and

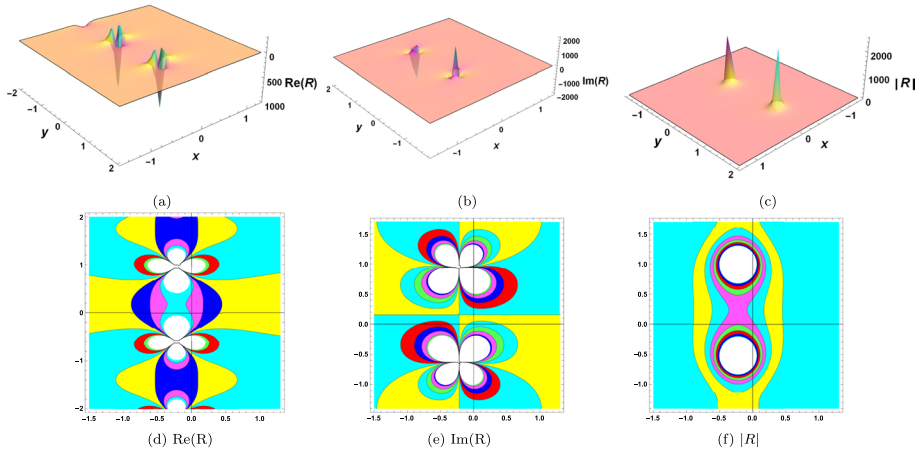

Fig. 4 Real, imaginary, and magnitude components of (49), highlighting the emergence of localized peaks and oscillatory symmetry

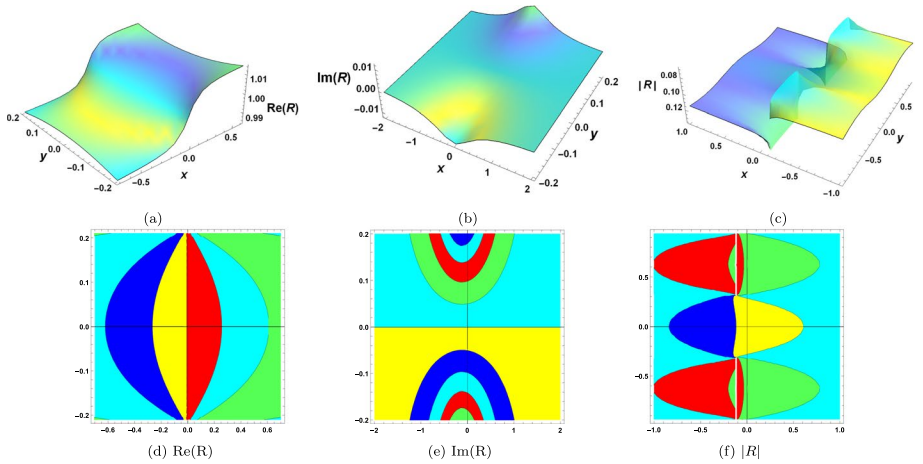

Fig. 5 Visual illustrations, incorporating 3D and contour graphs, of the real, imaginary, and magnitude components of (61)

$y \in [-0.94, 0.94]$, subgraphs (d) showing symmetrical oval patterns, (e) displaying layered, symmetrical curves and (f) contour plot of the magnitude of R with distinct symmetrical shapes indicating magnitude distribution.

- Within the context of solution (65), the graphical representation in Figure 6 demonstrates the various visual representations. The 3D plot in (a) shows the real part of the complex function R. The plot illustrates how $Re(R)$ varies across the x and y axes, displaying a sharp peak at the origin, indicating a significant variation in the real component in the region for $\omega_1 = 2$, $\omega_2 = 5i$, $\omega_3 = i$, $\omega_5 = 0$, $\mathcal{T}_0 = 1$, $\mathcal{T}_1 = 0$, $\mathcal{T}_2 = 0$, $\mathcal{K}_1 = 2$, $\mathcal{K}_2 = 0$, with time and spatial coordinates set to $t = 0.01$, $z = 0.02$ within the bounds of $x \in [-0.5, 0.4]$ and $y \in [-0.2, 0.2]$, The 3D plot in (b) shows a peak at the origin, suggesting a high concentration of imaginary values at this point for $\omega_1 = 2$, $\omega_2 = 5i$,

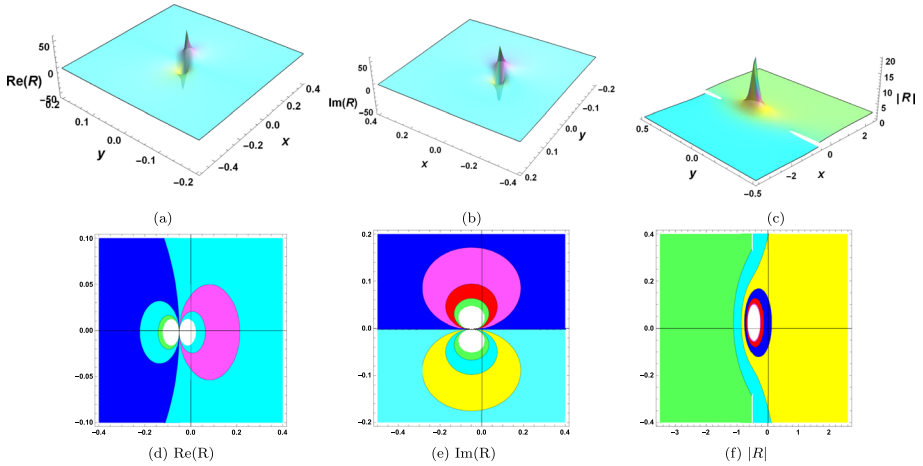

Fig. 6 Real, imaginary, and magnitude parts of (65), showing sharp localized peaks with oscillatory contour patterns that highlight symmetry in the solution

$\omega_3 = i, \omega_5 = 0, \mathcal{T}_0 = 1, \mathcal{T}_1 = 0, \mathcal{T}_2 = 0, \mathcal{K}_1 = 2, \mathcal{K}_2 = 0$, with time and spatial coordinates set to $t = 0.01, z = 0.02$ within the bounds of $x \in [-0.4, 0.4]$ and $y \in [-0.2, 0.2]$, The 3D plot in (c) represents the absolute value of the complex function, highlighting regions where the function's overall value is significant. The peak at the origin indicates a high magnitude at this point for $\omega_1 = 2$, $\omega_2 = 5i$, $\omega_3 = i$, $\omega_5 = 0$, $\mathcal{T}_0 = 1$, $\mathcal{T}_1 = 0$, $\mathcal{T}_2 = 0$, $\mathcal{K}_1 = 2$, $\mathcal{K}_2 = 0$, with time and spatial coordinates set to $t = 0.1, z = -0.02$ within the bounds of $x \in [-3.5, 2.6]$ and $y \in [-0.5, 0.5]$, while the contour plots (d), (e) and (f) offer a detailed view of these variations in two-dimensional planes.

- Figure 7, presents a set of graphical representations of the solution (69), including 3D surface plots, contour plots, and spherical plots, illustrating the real part and magnitude of a complex function *R*. The 3D surface plot in (a) shows the real part of the function *R*. This plot highlights the variation of *Re*(*R*) over the *x* and *y* axes, featuring a distinct depression near the origin, which indicates a region where the real part of the function reaches a minimum value for $\omega_1 = 2$, $\omega_2 = 2i$, $\omega_3 = i$, $\omega_5 = 0$, $\mathcal{T}_0 = 0$, $\mathcal{T}_1 = 0.01$, with time and spatial coordinates set to $t = 0.2, z = 0.2$ within the bounds of $x \in [-1, 0.2]$ and $y \in [-1.2, 0]$. The contour plot in (b) illustrates the real part *Re*(*R*) across the x and y planes. The concentric rings with varying colors represent different levels of *Re*(*R*), with the origin marked by a notable variation in color, indicating the minimum observed in the 3D plot for $\omega_1 = 2$, $\omega_2 = 2i$, $\omega_3 = i$, $\omega_5 = 0.3i$, $\mathcal{T}_0 = 0$, $\mathcal{T}_1 = 0.001$, with time and spatial coordinates set to $t = 1, z = 1$ within the bounds of $x \in [-1, 0.2]$ and $y \in [-1.4, 0.17]$. The spherical plot in (c) represents the real part *Re*(*R*) of the function *R* in spherical coordinates. This plot provides a three-dimensional visualization of how the real component of *R* varies in all directions from the origin, showing a symmetric pattern for $\omega_1 = 2$, $\omega_2 = 2i$, $\omega_3 = i$, $\omega_5 = 0$, $\mathcal{T}_0 = 0$, $\mathcal{T}_1 = 0.01$, with time and spatial coordinates set to $t = 0, z = 0$ within the bounds of $x \in [0, 2\pi]$ and $y \in [0, 2\pi]$, plot (d) demonstrates how *R* varies across the x and y axes, with notable peaks away from the origin, suggesting areas of significant magnitude in the function

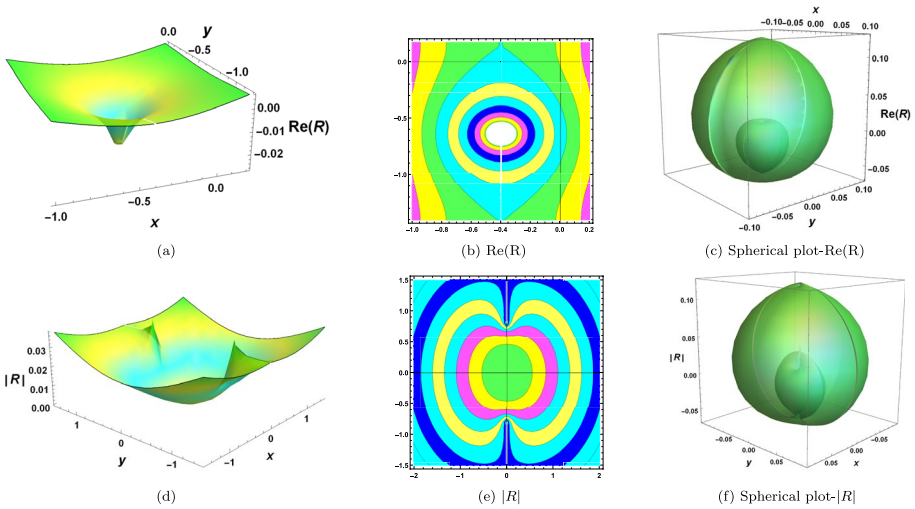

Fig. 7 Real and absolute components of (69), illustrating oscillatory distributions in 3D/contour form and spherical symmetry in intensity patterns

for $\omega_1 = 2, \omega_2 = 2i, \omega_3 = i, \omega_5 = 0, \mathcal{T}_0 = 0, \mathcal{T}_1 = 0.01$, with time and spatial coordinates set to $t = 0, z = 0$ within the bounds of $x \in [-1.5, 1.5]$ and $y \in [-1.5, 1.5]$, The plot (e) indicates higher magnitudes away from the origin for $\omega_1 = 2, \omega_2 = 2i, \omega_3 = i$, $\omega_5 = 0, \mathcal{T}_0 = 0, \mathcal{T}_1 = 0.01$, with time and spatial coordinates set to $t = 0, z = 0$ within the bounds of $x \in [-2, 2]$ and $y \in [-1.5, 1.5]$, plot (f) provides a 3-dimensional view of the magnitude variation in all directions, highlighting areas with significant values $\omega_1 = 2$, $\omega_2 = 2i$, $\omega_3 = i$, $\omega_5 = 0$, $\mathcal{T}_0 = 0$, $\mathcal{T}_1 = 0.01$, with time and spatial coordinates set to $t = 0, z = 0$ within the bounds of $x \in [0, 2\pi]$ and $y \in [0, 2\pi]$. The obtained solitonic structures, such as cone-shaped and apple-like profiles, have important implications in plasma physics and theoretical physics. Cone-shaped waveforms can be used to model localized plasma wave packets and nonlinear excitations that propagate stably without distortion in three spatial directions. Similarly, apple-like or spherical profiles can represent three-dimensional localized energy concentrations, which are relevant to plasma confinement, nonlinear optics, and fluid dynamics. These shapes resemble the propagation of multi-soliton and multi-peakon waves in magnetized plasma and can also provide insight into energy localization phenomena in nonlinear media. Such graphical solutions not only enrich the theoretical framework of soliton theory but also suggest potential applications in areas such as plasma wave modeling, nonlinear communication channels, and wave interactions in high-energy physics.

5 Conclusion

In conclusion, we extracted a wide range of solutions to a nonlinear (3+1)-D evolution equation using the newly proposed “generalized exponential rational integral function method," which has proven to be a powerful and innovative tool for extracting closed-form analytical solutions for highly nonlinear evolution equations. We obtained a wide range of solutions using GERIF, including exponential, trigonometric, hyperbolic, logarithmic, and inverse functions. These solutions had never been reported before. To provide a better understanding of these solutions, we have employed various visualizations, including 3D plots, contour plots, and spherical plots. These visualizations have shed light on the intricate patterns that emerge, such as lumps, peakons, solitons, periodic-lumps, periodic-peakons, symmetric patterns, periodic-solitons, and unique shapes like oval patterns, cone-shaped structures, and apple-like structures. These solutions can be applied in many areas, including light wave propagation in theoretical physics, wave behavior in fluids and plasmas, and various other fields.

5.1 Future scope

In this work, we constructed various solution sets to the (3+1)-D evolution equation, there are several future pathways for future research. Firstly, further exploration can be conducted to investigate the dynamic behavior and interactions of the identified solutions, such as lumps, peakons, solitons, periodic-lumps, periodic-peakons, periodic solitons, and symmetric patterns. Additionally, extending this method to tackle more complex nonlinear equations or higher dimensional systems could yield valuable insights into a broader range of mathematical and physical phenomena. Lastly, exploring potential applications in fields beyond

applied mathematics, such as plasma physics, engineering, or even data sciences, could open up new perspectives for the practical utilization of the discovered solutions. Overall, this work presents a promising foundation for future research endeavors with the potential to advance our understanding of nonlinear dynamics and their real-world implications.

Acknowledgements The author, Sachin Kumar, is extremely thankful for the financial support received from the Institution of Eminence at the University of Delhi, as detailed in the grant letter Ref. No./IoE/2025-26/12/FRP.

Author Contributions Shubham Kumar Dhiman and Monika Niwas wrote the article, supplied the methodology and visualization, and created the figures, whereas Sachin Kumar and Wen-Xiu Ma offered the validation, formal analysis, conception, methodology, research, and supervision. M.A. Abdou provided the visualization and formal analysis. All authors have approved and consented to the publication of this research article.

Funding None.

Data Availability No datasets were generated or analysed during the current study.

Declarations

Competing interests The authors declare no competing interests.

Ethics approval and consent to participate This is not applicable to this manuscript.

Conflicts of Interest The authors state that there are no conflicts of interest.

References

1. Günhan A.N., Zehra. T., Yaşar, E.: Exact soliton solutions of the perturbed nonlinear Schrödinger equation with conformable fractional derivative by two distinct methods. Modern Phys. Lett. B. 2550226 (2025). https://doi.org/10.1142/S0217984925502264
2. Seadawy, A.R., Ali, A., Bekir, A., Cevikel,A.C.: Advanced techniques for analyzing solitary wave solutions of the generalized fractional Kundu–Mukherjee–Naskar model. Modern Phys. Lett. B. 2550224 (2025). https://doi.org/10.1142/S0217984925502240
3. Kudryashov, N.A.: Solitary waves of burgers hierarchy equations. Computat. Math. Math. Phys. **65**, 995–1003 (2025)
4. Ma, W.X., Zhou, Y.: Lump solutions to nonlinear partial differential equations via hirota bilinear forms. J. Differential Equations **264**(4), 2633–2659 (2018)
5. Hosseini, K., Samavat, M., Mirzazadeh, M., Ma, W.X., Hammouch, Z.: A new (3 + 1)-dimensional hirota bilinear equation: its bäcklund transformation and rational-type solutions. Regular Chaotic Dyn. **25**(4), 383–391 (2020)
6. Dehghan, M., Heris, J.M., Saadatmandi, A.: Application of the exp-function method for solving a partial differential equation arising in biology and population genetics. Int. J. Numer. Methods Heat Fluid Flow. **21**(6), 736–753 (2011)
7. Wazwaz, A.M.: New (3 + 1)-dimensional painlevé integrable fifth-order equation with third-order temporal dispersion. Nonlinear Dyn. **106**, 891–897 (2021)
8. Xu, G.Q., Wazwaz, A.M.: A new (n+1)-dimensional generalized kadomtsev-petviashvili equation: integrability characteristics and localized solutions. Nonlinear Dyn. **111**, 9495–9507 (2023)
9. Zhao, Y.W., Xia, J., W., Lu, X.: The variable separation solution, fractal and chaos in an extended coupled (2+1)-dimensional Burgers system. Nonlinear Dyn. **108**, 4195–4205 (2022)
10. He, J.H.: Application of homotopy perturbation method to nonlinear wave equations. Chaos, Solitons Fractals **26**(3), 695–700 (2005)

11. Dehghan, M., Heris, J.M., Saadatmandi, A.: Application of semi-analytic methods for the fitzhugh-nagumo equation, which models the transmission of nerve impulses. Math. Methods Appl. Sci. **33**(11), 1384–1398 (2010)
12. Kumar, S., Niwas, M.: Exploring lump soliton solutions and wave interactions using new inverse (g'/g)-expansion approach: applications to the (2+1)-dimensional nonlinear heisenberg ferromagnetic spin chain equation. Nonlinear Dyn. **111**(21), 20257–20273 (2023)
13. Kumar, S., Niwas, M.: Analyzing multi-peak and lump solutions of the variable-coefficient boiti–leon–manna–pempinelli equation: a comparative study of the lie classical method and unified method with applications. Nonlinear Dyn. **111**(24), 22457–22475 (2023)
14. Mubaraki, A.M., Nuruddeen, R.I., Ali, K.K., Gómez-Aguilar, J.F.: Additional solitonic and other analytical solutions for the higher-order boussinesq-burgers equation. Opt. Quantum Electron. **56**(2), 165 (2024)
15. Althobaiti, S., Nuruddeen, R.I., Magaji, A.Y., Gómez-Aguilar, J.F.: New revelations and extensional study on the recent sixth-order 3-d kadomtsev-petviashvili-sawada-kotera-ramani equation. Opt. Quantum Electron. **56**(5), 820 (2024)
16. Abdullah, Rahman, G.U., Gómez-Aguilar, J.F.: M-shape, lump, homoclinic breather and other soliton interaction of the Landau-Ginzburg-Higgs model in nonlinear fiber optics. Chaos Solitons Fractals **196**, 116335 (2025)
17. Rahman, G.U., Abdullah, Meetei, M.Z., Gómez-Aguilar, J.F.: Investigation of the dynamical perspective of soliton solutions to the (3+1)-dimensional Boussinesq model using two distinctive methods. Nonlinear Dyn. **113**(18), 25097–25119 (2025)
18. Hirota, R.: The Direct Method in Soliton Theory, Cambridge University Press, (2004)
19. Kumar, S., Mohan, B., Kumar, R.: Lump, soliton, and interaction solutions to a generalized two-mode higher-order nonlinear evolution equation in plasma physics. Non-linear Dyn. **110**, 693–704 (2022). https://doi.org/10.1007/s11071-022-07647-5
20. Dhiman, S.K., Kumar, S.: Different dynamics of invariant solutions to a generalized (3+1)-dimensional camassa-holm-kadomtsev-petviashvili equation arising in shallow water-waves. J. Ocean Eng. Sci. (2022). https://doi.org/10.1016/j.joes.2022.06.019
21. Seyedi, S., H., Saray, B., N., Nobari, M., R., H.: Using interpolation scaling functions based on Galerkin method for solving non-newtonian fluid flow between two vertical flat plates. Appl. Math. Comput. **269**, 488–496 (2015)
22. Niwas, M., Kumar, S., Rajput, R., Chadha, D.: Exploring localized waves and different dynamics of solitons in (2 + 1)-dimensional hirota bilinear equation: a multivariate generalized exponential rational integral function approach. Nonlinear Dyn. **112**(11), 1–14 (2024)
23. Günhan Ay, N., Yaşar, E.: A new (3+1) dimensional hirota bilinear equation: painlavé integrability, lie symmetry analysis, and conservation laws. J. Taibah University Sci. **16**(1), 1287–1297 (2022)
24. Ismael, H.F., Nabi, H.R., Sulaiman, T.A., Shah, N.A., Eldin, S.M., Bulut, H.: Hybrid and physical interaction phenomena solutions to the hirota bilinear equation in shallow water waves theory. Results Phy. **53**, 106978 (2023)
25. Ghanbari, B., Inc, M.: A new generalized exponential rational function method to find exact special solutions for the resonance nonlinear schrödinger equation. Eur. Phys. J. Plus. **133**, 142 (2018)
26. Ma, W.X., Huang, T.W., Zhang, Y.: A multiple exp-function method for nonlinear differential equations and its application. Phys. Scripta. **82**(6), 065003 (2010)

Authors and Affiliations

Shubham Kumar Dhiman[1] · Monika Niwas[2] · Sachin Kumar[1] · Wen-Xiu Ma[3,4] · M. A. Abdou[5,6]

✉ Sachin Kumar
sachinambariya@gmail.com

✉ Wen-Xiu Ma
mawx@cas.usf.edu

[1] Department of Mathematics, Faculty of Mathematical Sciences, University of Delhi, Delhi 110007, India

[2] Department of Mathematics, Shyama Prasad Mukherji College for Women, University of Delhi, Delhi 110026, India

[3] Department of Mathematics and Statistics, University of South Florida, Tampa, FL 33620, USA

[4] Research Center of Astrophysics and Cosmology, Khazar University, 41 Mehseti Street, Baku 1096, Azerbaijan

[5] Department of Physics, College of Science, University of Bisha, P.O Box 344, Bisha 61922, Saudi Arabia

[6] Theoretical Research Group, Physics Department, Faculty of Science, Mansoura University, Mansoura 35516, Egypt